



Comparative study on electrospun magnesium silicate ceramic fibers fabricated through two synthesis routes



Chonghe Xu, Shuying Shi, Silun Zhu, Xiaoqian Zhang, Xinqiang Wang*, Luyi Zhu, Guanghui Zhang

State Key Laboratory of Crystal Materials and Institute of Crystal Materials, Shandong University, Jinan 250100, PR China

ARTICLE INFO

Article history:

Received 13 February 2020
Received in revised form 10 April 2020
Accepted 15 April 2020
Available online 18 April 2020

Keywords:

Microstructure
Thermal analysis
Magnesium silicate
Ceramic fibers
Electrospinning

ABSTRACT

We report two routes for the electrospinning of magnesium silicate ceramic fibers (MSCFs) using different precursor solutions involving different magnesium sources and synthesis procedures. The thermal decomposition processes and microstructure of the MSCFs were comparatively studied. X-ray diffraction results confirmed the crystalline MgSiO_3 phase in the heat-treated fibers. Magnesium sol contained precursor supplied long and straight MSCFs with homogeneous microstructure. Magnesium chloride contained precursor produced coiled or spring-like MSCFs with core-shell structure. The formation mechanism of the unique structure of C2-1000 was briefly analyzed. In addition, true density and specific surface area of MSCFs, and thermal conductivity of fiber tablets were measured. The reported methods can be extended as a general approach to prepare other silicate ceramic fibers.

© 2020 Elsevier B.V. All rights reserved.

1. Introduction

Oxide ceramic fibers (OCFs) are materials of light weight and thermal stability, which are widely used for high-temperature filtration and insulation [1]. The most widely used refractory ceramic fibers (RCFs) are SiO_2 , Al_2O_3 and $\text{SiO}_2\text{-Al}_2\text{O}_3$ fibers [2]. Sometimes oxides such as ZrO_2 , Cr_2O_3 are added to achieve specific properties [3]. Benefit from the reinforcement of OCFs, the ceramic matrix composites (CMCs) obtain excellent heat resistance, creep resistance and thermal shock resistance, and are applied in aerospace engineering, biomedical and electronic devices [4].

Alkaline earth silicate fibers are newly-developing RCFs which have low potential threat to health due to their good biological solubility [5]. Compared with traditional melt-spinning, centrifugal spinning and solution blowing spinning method [6,7], electrospinning technique combined with sol-gel method can controllably produce ultrafine fibers with diverse structure and small diameter dispersion coefficient. Magnesium silicate ceramic fibers (MSCFs) are harmless to human body, have small bulk density and low thermal conductivity, and can be used as substitute for carcinogenic aluminum silicate ceramic fibers. However, the fabrication of MSCFs by electrospinning remains a challenge due to the technical difficulty in spinning sol synthesis.

In this work, two strategies toward the electrospinning fabrication of MSCFs are developed by virtue of two types of precursor

solution. One strategy is using citric acid as the ligand to synthesize the magnesium sol before adding silica sol, the other is adding strong acid type inorganic magnesium salt to the silica sol. MSCFs obtained by the two routes were characterized and compared to understand their different features.

2. Methodology

2.1. Synthesis of spinning solution

Silica sol was prepared by adding 20 g H_3PO_4 solution ($n(\text{H}_3\text{PO}_4\text{-H}_2\text{O}):n(\text{H}_2\text{O}):n(\text{EtOH}) = 0.01:6:2$) into 20.83 g $\text{Si}(\text{OC}_2\text{H}_5)_4$ (TEOS) dropwise with stirring for 3 h. 6 wt% PVA (polyvinyl alcohol, MW = 88,000) solution was prepared with 30 wt% EtOH. The synthesis method was described as a Si:Mg ratio of 2:1.

Route A: Magnesium sol was prepared by dissolving MgO into 50 wt% citric acid solution as $n(\text{MgO}:\text{C}_6\text{H}_8\text{O}_7\text{-H}_2\text{O}) = 1:3$. Then, 8 g silica sol was added dropwise into 8.8 g magnesium sol with stirring for 30 min; 12.4 g 6 wt% PVA solution was subsequently added dropwise and stirring for 2 h.

Route B: Firstly, 2.54 g $\text{MgCl}_2\cdot 6\text{H}_2\text{O}$ was dissolved into 20 g silica sol to obtain Si-Mg sol. Secondly, 20 g 6 wt% PVA solution was added dropwise to Si-Mg sol and stirring for 2 h.

2.2. Electrospinning and heat-treatment

The electrospinning process was performed at ambient temperature of 20–35 °C and humidity of 30–50%. Spinning process

* Corresponding author.

E-mail address: xqwang@sdu.edu.cn (X. Wang).

parameters: 15 kV voltage, receiving distance of 20 cm, and feeding rate of $1.0 \text{ mL}\cdot\text{h}^{-1}$. Fibers obtained by route A and B were labeled as M8 and C2, respectively. The as-spun fibers were then heat-treated in a muffle furnace, firstly heated to $400 \text{ }^\circ\text{C}$ for 1 h by $2 \text{ }^\circ\text{C}/\text{min}$, and then $5 \text{ }^\circ\text{C}/\text{min}$ to target temperature.

2.3. Characterizations

Simultaneous thermogravimetry and differential scanning calorimetry (TG/DSC, NETZSCH STA 449F5, Germany) measurements were performed at a heating rate of $10 \text{ }^\circ\text{C}/\text{min}$ in air. X-ray diffractions (XRD, D8 Advance, Bruker, Germany) were operated with Cu-K α radiation. Scanning electron microscope (SEM, S-4800, Hitachi, Japan) was conducted with an acceleration voltage of 5 kV. The diameter data were obtained by a software named Nano Measurer. Transmission electron microscopy (TEM) and element mapping (JEOLJEM-2100F, Japan) were operated at 200 kV. N_2 adsorption-desorption isotherms (JW-BK112, JWGB Sci&Tech, China) were measured at 77 K. True density of fibers was measured by a full-automatic true density tester (JW-M100, JWGB Sci&Tech, China). Fiber tablets ($4 \times 4 \times 1 \text{ mm}$) were prepared for thermal conductivity test using laser flash method (NETZSCH LFA457, Germany). Concretely, fibers were grinded with 5% PVA solution gently and 0.3 g mixture was infused in a mold with a uniaxial press of 8 MPa, and finally calcined at $800 \text{ }^\circ\text{C}$ to remove off the PVA. The porosity of the tablets was measured by the Archimedes method.

3. Results and discussions

The TG curve of M8 (Fig. 1(a)) contained two weight loss stages. The first stage below $260.5 \text{ }^\circ\text{C}$ was attributed to the elimination of moistures and the preliminary oxidation of precursors [8]. The second stage ($260.5\text{--}682.6 \text{ }^\circ\text{C}$) comprised a large exothermic peak at $497.5 \text{ }^\circ\text{C}$ in DSC curve, which was ascribed to the pyrolysis of PVA main chain, citrate and carbonate intermediates [9,10]. At higher temperature region, negligible weight loss was caused

mainly by the evaporated water molecules coming from the self-condensation reaction of silanol groups [11]. The small exothermic peak at $884.9 \text{ }^\circ\text{C}$ in the DSC curve was associated with the crystallization of magnesium silicate. The weight loss of C2 was divided into three stages (Fig. 1(b)). The first stage was the removal of trapped solvent and crystalline water. The other two stages were the removal of trapped solvents, the dehydration of silane groups, and the decomposition of the PVA side chains [10,11]. In the DSC curve, endothermic peaks at $133.8 \text{ }^\circ\text{C}$ and $169.8 \text{ }^\circ\text{C}$ were due to the loss of crystalline water from $\text{MgCl}_2\cdot 6\text{H}_2\text{O}$ [12]. Another endothermic peak at $463.1 \text{ }^\circ\text{C}$ was the form of MgO. The wide exothermic peak at $889.2 \text{ }^\circ\text{C}$ belonged to the pyrolysis of silane groups and the crystallization of MgSiO_3 . The total weight loss of M8 (75.78%) was larger than that of C2 (58.03%), which was due to the large amount of citrate in M8.

The broad peak around $2\theta = 20\text{--}30^\circ$ in XRD patterns of fibers treated at different temperatures indicated the existence of amorphous SiO_2 . M8 was amorphous after heat-treated at $800 \text{ }^\circ\text{C}$, while it began to form crystalline MgSiO_3 at $850 \text{ }^\circ\text{C}$ (Fig. 1(c)). As for C2, periclase MgO (PDF#45-0946) crystallized after heat-treated at $700 \text{ }^\circ\text{C}$, MgSiO_3 crystallized also at $850 \text{ }^\circ\text{C}$, while MgO still existed after heat-treated at $1000 \text{ }^\circ\text{C}$ (Fig. 1(e)). MgSiO_3 in both M8-1000 and C2-1000 (heat-treated at $1000 \text{ }^\circ\text{C}$) consisted of clinoenstatite (PDF#35-0610) and orthorhombic perovskite (PDF#19-0768).

The MSCFs fabricated by A and B routes showed dissimilar geometries. M8-1000 was straight fiber with cylindrical shape, large aspect ratio (Fig. 2(a, b)) and an averaged diameter of $1.16 \text{ }\mu\text{m}$ (Fig. 2(i)). The surface of M8-1000 was not very smooth and the entire fiber was the accumulation of fine particles (Fig. 2(c, d)). Seen from TEM image (Fig. 2(j)) and element mapping (Fig. 2(m)), both the structure and composition of M8 were homogeneous, indicating the good hybridization of Si and Mg in precursor sol. However, the C2-1000 fibers were curved, intertwined with each other, and some coiled fibers were in spring-like shape (Fig. 2(e, f)). The unique morphology of C2-1000 might be caused by the violent whipping process of the jet due to the high solution conductivity of 10.78 m S/cm (Table 1). C2-1000 showed regular cylin-

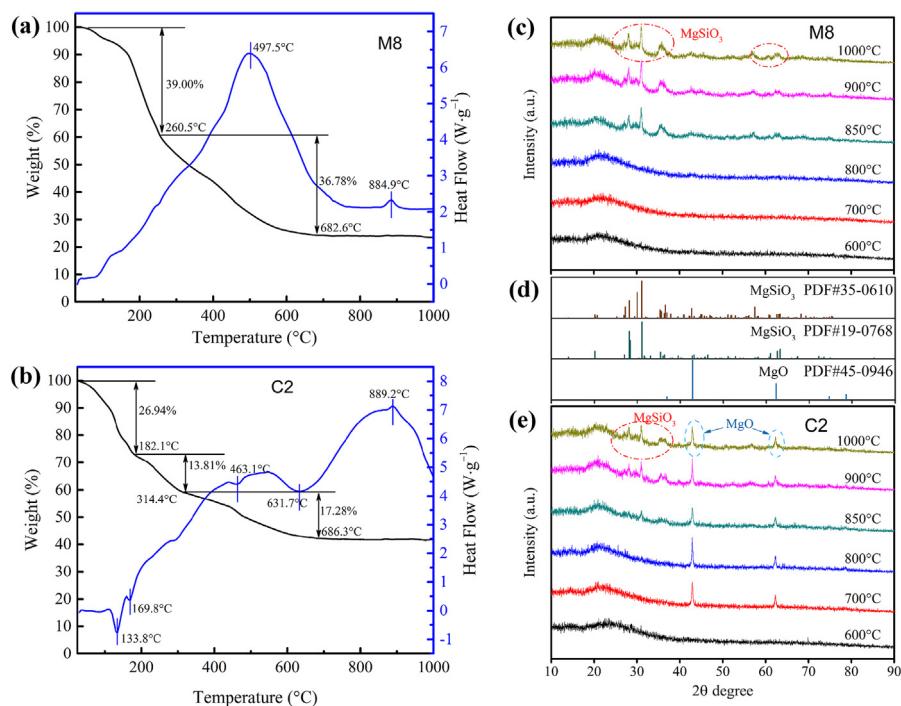


Fig. 1. TG-DSC curves of M8 (a) and C2 (b) recorded in air; XRD patterns of M8 (c) and C2 (e) after heat-treated for 2 h at different temperatures; standard PDF cards (d).

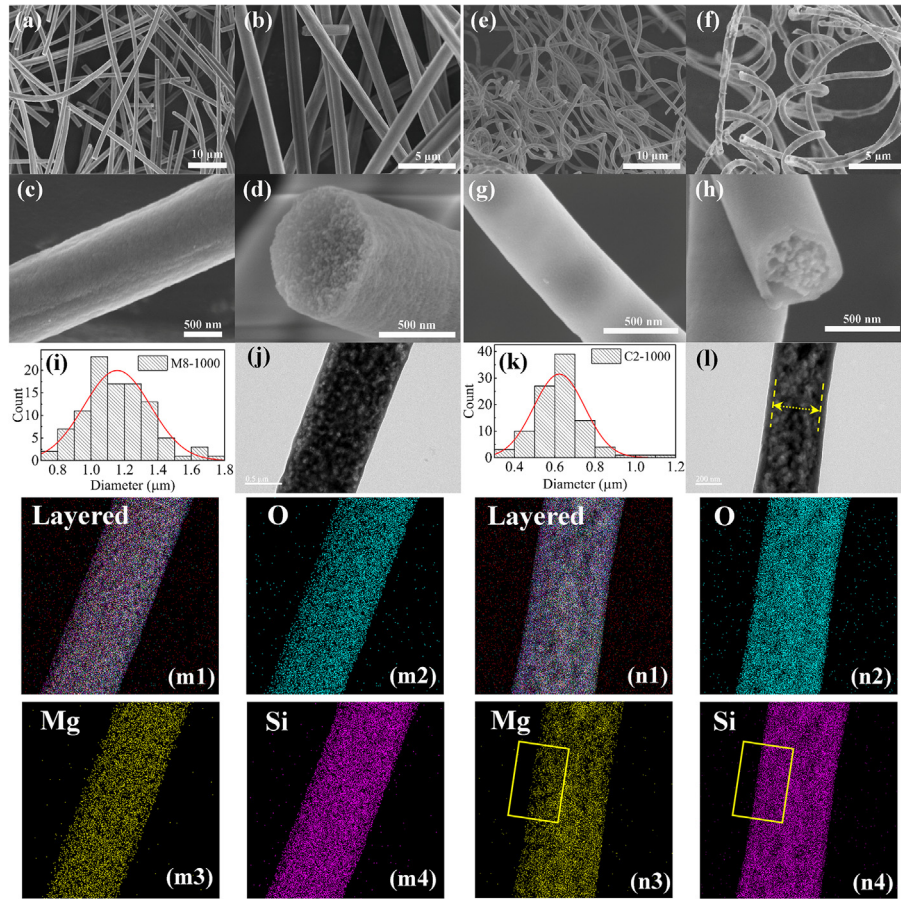


Fig. 2. SEM images of M8-1000 (a-d) and C2-1000 (e-h); diameter distribution of M8-1000 (i) and C2-1000 (k); TEM images of M8-1000 (k) and C2-1000 (l); element mapping of M8-1000 (m1-4) and C2-1000 (n1-4).

Table 1
Related parameters of fibers and fiber tablets.

Sample form		M8	C2
Spinning sol	Conductivity (m S/cm)	1.72	10.78
	pH value	2.63	2.24
	Surface Intensity (mN m)	32.90	29.86
	Viscosity (mPa s)	156.6	225.8
Fiber*	True density (g/cm ³)	3.9281	4.2527
	S_{BET} (m ² /g)	8.535	7.879
	Averaged diameter (μm)	1.157	0.622
	Apparent density (g/cm ³)	0.188	0.142
Tablet*	Porosity (%)	15.59	39.33
	Thermal conductivity (W/(m·K), 25 °C)	0.137	0.134

*Measured from fibers heat-treated at 1000 °C for 2 h or tablets made by them.

drical shape and smooth surface (Fig. 2(g)) with an averaged diameter of 0.62 μm (Fig. 2(k)). The cross-sectional SEM image and typical TEM image (Fig. 2(h, l)) revealed that C2-1000 was core-shell structured with internal granular structure and dense surface layer. The marked box in Fig. 2(n1-n4) showed that Mg content was obviously lower at the edge, while the distribution of Si was uniform. The core-shell structure of C2-1000 could be attributed to the higher migration rate of Si than Mg toward outer surface during heat-treatment process [13]. Besides, the coiled fiber C2-1000 with special spring-like morphology had potential applications in composite materials, sensor device and tissue engineering [14–16], which might be an attractive issue in further research.

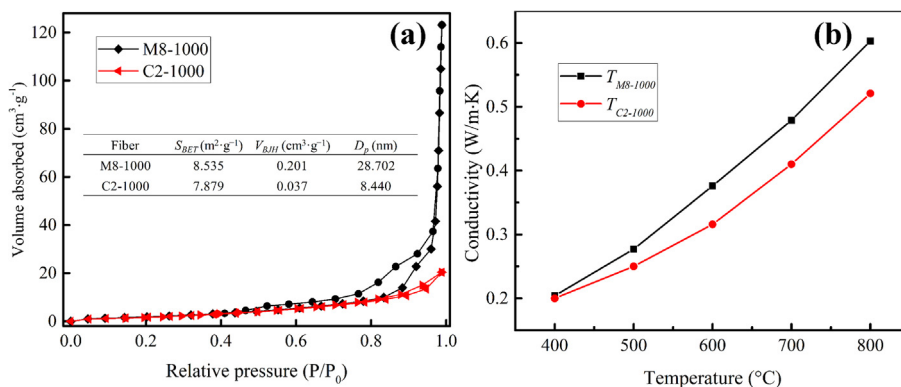


Fig. 3. Nitrogen adsorption desorption isotherm (a) and thermal conductivity (b) of tablets pressed by M8-1000 and C2-1000.

As shown in Table 1, the true density of C2-1000 (4.2527 g/cm³) was higher than M8-1000 (3.9281 g/cm³), which was in accordance with a lower specific surface area (S_{BET}) of 7.879 m²/g than that of 8.535 m²/g for M8-1000. In Fig. 3(a), M8-1000 showed a type-IV isotherm with H3 type hysteresis loop, suggesting the slit-shaped pores formed. The thermal conductivity at room temperature (Table 1) of fiber tablets M8-1000 ($T_{M8-1000}$) and C2-1000 ($T_{C2-1000}$) were 0.137 and 0.134 W/(m·K), respectively. Fig. 3 (b) showed that the thermal conductivity of $T_{M8-1000}$ and $T_{C2-1000}$ increased from 0.200 to 0.603 W/(m·K) at higher temperatures of 400–800 °C. The porosity of $T_{M8-1000}$ was lower than $T_{C2-1000}$, which was reasonable for a higher thermal conductivity of $T_{M8-1000}$.

4. Conclusion

Two strategies have been developed for the fabrication of MSCFs by electrospinning and heat-treatment. Fibers prepared with magnesium source of MgCl₂·6H₂O showed a lower crystallization temperature than those prepared with citrate due to MgO crystallized firstly. Crystalline MgSiO₃ was formed in both fibers after heat-treatment at 850 °C. M8-1000 was straight long fiber with homogeneous polycrystalline structure. C2-1000 was coiled or spiral fiber with dense surface and polycrystalline interior. Precursor type and thermal decomposition process had substantial impact on the geometry and microstructure of the ceramic fibers. M8-1000 possessed lower true density and higher S_{BET} than C2-1000. The thermal conductivities of fiber tablets were 0.200–0.603 W/(m·K) at 400–800 °C. The MSCFs produced in this work have considerable potential in thermal insulation and related applications.

CRedit authorship contribution statement

Chonghe Xu: Conceptualization, Methodology, Writing - original draft. **Shuying Shi:** Data curation, Writing - review & editing. **Silun Zhu:** Software, Visualization. **Xiaoqian Zhang:** Validation. **Xinqiang Wang:** Supervision, Writing - review & editing, Project administration, Funding acquisition. **Luyi Zhu:** Funding acquisition. **Guanghui Zhang:** Resources.

Declaration of Competing Interest

The authors declare that they have no known competing financial interests or personal relationships that could have appeared to influence the work reported in this paper.

Acknowledgments

This work was supported by the National Natural Science Foundations of China (Grant Nos. 51372140, 51472144), Shandong University Young Scholars Program (2016WLJH27) and the Fundamental Research Funds for the Central Universities (Grant No. 2082019014).

References

- [1] L. Li, W. Kang, Y. Zhao, Y. Li, J. Shi, B. Cheng, Ceram. Int. 41 (2015) 409–415, <https://doi.org/10.1016/j.ceramint.2014.08.085>.
- [2] A.R. Bunsell, M.-H. Berger, J. Eur. Ceram. Soc. 20 (2000) 2249–2260, [https://doi.org/10.1016/S0955-2219\(00\)00090-X](https://doi.org/10.1016/S0955-2219(00)00090-X).
- [3] M.J. Utell, L.D. Maxim, Toxicol. appl. pharm. 361 (2018) 113–117, <https://doi.org/10.1016/j.taap.2018.06.011>.
- [4] J. Silvestre, N. Silvestre, J. de Brito, J. Nanomater. 2015 (2015) 1–13, <https://doi.org/10.1155/2015/106494>.
- [5] R.C. Brown, P.T. Harrison, Regul. toxicol. pharm. 64 (2012) 296–304, <https://doi.org/10.1016/j.yrtph.2012.08.020>.
- [6] R.M.d.C. Farias, R.R. Menezes, J.E. Oliveira, E.S. de Medeiros, Mater. Lett. 149 (2015) 47–49. doi: 10.1016/j.matlet.2015.02.111.
- [7] M.D. Calisir, A. Kilic, Mater. Lett. 258 (2020) 126751, <https://doi.org/10.1016/j.matlet.2019.126751>.
- [8] A. Mahapatra, B.G. Mishra, G. Hota, J. Hazard. Mater. 258–259 (2013) 116–123, <https://doi.org/10.1016/j.jhazmat.2013.04.045>.
- [9] B.M. Abu-Zied, A.M. Asiri, Thermochim. Acta 649 (2017) 54–62, <https://doi.org/10.1016/j.tca.2017.01.003>.
- [10] C. Shao, H.-Y. Kim, J. Gong, B. Ding, D.-R. Lee, S.-J. Park, Mater. Lett. 57 (2003) 1579–1584, [https://doi.org/10.1016/S0167-577X\(02\)01036-4](https://doi.org/10.1016/S0167-577X(02)01036-4).
- [11] S.-S. Choi, S.G. Lee, J. Mater. Sci. Lett. 22 (2003) 891–893, <https://doi.org/10.1023/A:1024475022937>.
- [12] Q. Huang, G. Lu, J. Wang, J. Yu, J. Anal. Appl. Pyrolysis 91 (2011) 159–164, <https://doi.org/10.1016/j.jaap.2011.02.005>.
- [13] Z. Du, L. Guo, T. Zheng, Q. Cai, X. Yang, Ceram. Int. 45 (2019) 23975–23983, <https://doi.org/10.1016/j.ceramint.2019.08.099>.
- [14] W. Feng, J. Li, Y. Feng, M. Qin, RSC Adv. 4 (2014) 10090, <https://doi.org/10.1039/c3ra45647a>.
- [15] C. Deng, L. Pan, D. Zhang, C. Li, H. Nasir, Nanoscale 9 (2017) 16404–16411, <https://doi.org/10.1039/c7nr05486f>.
- [16] S. Fleischer, R. Feiner, A. Shapira, J. Ji, X. Sui, H. Daniel Wagner, T. Dvir, Biomaterials 34 (2013) 8599–8606. Doi: 10.1016/j.biomaterials.2013.07.054.